Low-energy inelastic collisions of OH radicals with He atoms and D$_2$ molecules

Moritz Kirste,[1] Ludwig Scharfenberg,[1] Jacek Kłos,[2] François Lique,[3] Millard H. Alexander,[4]
Gerard Meijer,[1] and Sebastiaan Y. T. van de Meerakker[1]

[1]*Fritz-Haber-Institut der Max-Planck-Gesellschaft, Faradayweg 4-6, D-14195 Berlin, Germany*
[2]*Department of Chemistry and Biochemistry, University of Maryland, College Park, Maryland 20742-2021, USA*
[3]*LOMC, Université du Havre, 25 Rue Philippe Lebon, Boîte Postale 540-76 058, Le Havre Cedex, France*
[4]*Department of Chemistry and Biochemistry and Institute for Physical Science and Technology,*
University of Maryland, College Park, Maryland 20742-2021, USA

We present an experimental study on the rotational inelastic scattering of OH ($X\,^2\Pi_{3/2}, J = 3/2, f$) radicals with He and D$_2$ at collision energies between 100 and 500 cm^{-1} in a crossed beam experiment. The OH radicals are state selected and velocity tuned using a Stark decelerator. Relative parity-resolved state-to-state inelastic scattering cross sections are accurately determined. These experiments complement recent low-energy collision studies between trapped OH radicals and beams of He and D$_2$ that are sensitive to the total (elastic and inelastic) cross sections [Sawyer *et al.*, Phys. Rev. Lett. **101**, 203203 (2008)], but for which the measured cross sections could not be reproduced by theoretical calculations [Pavlovic *et al.*, J. Phys. Chem. A **113**, 14670 (2009)]. For the OH-He system, our experiments validate the inelastic cross sections determined from rigorous quantum calculations.

PACS number(s): 34.50.Ez, 37.10.Mn

I. INTRODUCTION

The study of collisions between neutral atoms and molecules at low collision energies is a fast developing field in molecular physics [1–5]. This growing interest originates from the exotic scattering properties of molecules at low temperatures. At temperatures below ∼10 K only a few partial waves contribute to the scattering, leading to dramatic changes in the dynamics. Scattering resonances can occur when the collision energy is degenerate with a bound state of the collision complex [6]. Low collision energies also allow for external control over the collision dynamics by electromagnetic fields. At collision energies below a few kelvin, the perturbations due to the Zeeman and Stark effect become comparable to the translational energy, opening the possibility for controlled chemistry [7].

In recent years, a variety of novel experimental methods have been developed that enable scattering experiments at lower collision energies and/or with a higher precision than hitherto possible. The buffer-gas cooling, the Stark deceleration, and the velocity selection techniques have already successfully been applied to molecular scattering experiments [8–11]. In the ultracold regime, spectacular advances have been made in the study of interactions between alkali-metal dimers near quantum degeneracy [12,13]. Together with the collection of other techniques that are currently being developed, these methods have the potential to start a new era in molecular scattering experiments.

The Stark deceleration technique has excellent potential for precise molecular scattering studies as a function of the collision energy. Compared to conventional molecular beam sources, a Stark decelerator produces beams of molecules with a narrow velocity spread, perfect quantum state purity, and with a computer controlled velocity [14]. So far, two experimental approaches have been followed to use these monochromatic beams in molecular scattering studies.

In 2006, the first scattering experiment using a Stark decelerated molecular beam was performed. Stark-decelerated OH radicals were scattered with a supersonic beam of Xe atoms under 90° angle of incidence [10]. This crossed molecular beam configuration allowed the accurate measurement of the relative inelastic scattering cross sections as a function of the collision energy in the collision energy range of 50 to 400 cm^{-1}. Recently, this experimental approach was improved significantly using a superior Stark decelerator [15]. With this decelerator, scattering experiments can be performed with a better sensitivity, as has been demonstrated for the benchmark OH($^2\Pi$)-Ar system [16]. In both experiments, excellent agreement was obtained with cross sections determined by quantum close-coupling calculations based on high-quality *ab initio* OH-Xe and OH-Ar potential energy surfaces (PES's).

In another experiment, the approach to confine the Stark-decelerated OH radicals in a permanent magnetic trap prior to the collision was followed [17]. Collisions with the OH radicals were studied by sending supersonic beams of He atoms or D$_2$ molecules through the trap. Information on the total collision cross sections could be inferred from the beam-induced trap loss that occurs through elastic as well as inelastic collisions. The collision energy was varied from 60 to 230 cm^{-1} for collisions with He and from 145 to 510 cm^{-1} for collisions with D$_2$ by changing the temperature of the pulsed solenoid valve used to produce the supersonic beams. Absolute collision cross sections were determined by calibrating the beam flux using a pressure measurement. Indications for quantum threshold scattering at a collision energy of 84 cm^{-1}, equal to the energy splitting of the two lowest lying rotational levels of the OH radical, were found for collisions between OH and He. For OH-D$_2$ collisions, a pronounced peak in the total cross section was observed at collision energies around 305 cm^{-1}, an energy that is equal to the energy splitting between the $J = 1$ and the $J = 3$ rotational levels of para-D$_2$. The enhancement of the cross section at this energy was tentatively attributed to resonant energy transfer between the OH radicals and D$_2$ molecules.

Both experimental approaches have been successful in demonstrating the feasibility of using Stark decelerated

molecules in scattering experiments. The experimental results of the latter experiment, however, could not be reproduced by theoretical calculations. The decrease in the total cross section that was observed below 84 cm^{-1} for the scattering between OH and He was not reproduced by rigorous quantum calculations for low temperature collisions of OH-He. The calculations show that the total cross section *increases* significantly at collision energies below 100 cm^{-1} [18]. The experimentally observed threshold behavior can be explained if the trap loss originates mainly from inelastic scattering, although this appears unlikely for the kinetic conditions of the experiment. The measured cross section of $\sim$100 Å^2 at a collision energy of 150 cm^{-1} is an order of magnitude larger than the theoretical total inelastic cross section, indicating that the majority of the collisions that lead to trap loss are indeed elastic. The source of the discrepancy between theory and experiment, and whether or not the presence of the trapping field in the collision experiment can explain the observed cross sections, is at present unclear. Unfortunately, no rigorous quantum calculations are available for the OH-D$_2$ system to compare calculated cross sections with experimental ones, or to investigate the physical origin of the intriguing peak that was observed at a collision energy of 305 cm^{-1}.

Here we complement the low-energy collision studies between OH-He and OH-D$_2$ of Sawyer *et al.* [17] by investigating rotational energy transfer in collisions of Stark-decelerated OH ($X\,^2\Pi_{3/2}, J = 3/2, f$) radicals with He atoms and D$_2$ molecules in a crossed beam experiment under field free conditions. The OH-He and OH-D$_2$ center-of-mass collision energies are tuned from 120 cm^{-1} to 400 cm^{-1} and from 150 cm^{-1} to 500 cm^{-1}, respectively. Parity-resolved state-to-state relative inelastic scattering cross sections are accurately measured. For the OH-He system, good agreement is obtained with the inelastic cross sections determined by close-coupled calculations based on the OH-He PES's used in Ref. [18], validating the theoretical predictions for the low-energy inelastic scattering between OH radicals and He atoms. For the OH-D$_2$ system, no strong variation in the state-to-state relative inelastic scattering cross sections is found at center-of-mass energies around 300 cm^{-1}.

The interaction of OH radicals with, in particular, He atoms has been the subject of extensive experimental and theoretical investigations, and is of direct astrophysical relevance. The rotational energy transfer of OH by collisions with H$_2$ molecules in interstellar clouds is believed to play an important role in the formation of interstellar OH masers [19]. The (mass scaled) collision cross sections for the theoretically more tractable OH-He system are often used to model the collision dynamics in these environments. In a crossed beam experiment, Schreel *et al.* prepared the OH radicals in the upper Λ-doublet component of the $X\,^2\Pi_{3/2}, J = 3/2$ level by hexapole state selection [20]. Accurate state-to-state inelastic scattering cross sections were obtained at a collision energy of $\sim$400 cm^{-1}. The effect of vibrational excitation of the OH radical on the rotational energy transfer has been investigated by Wysong *et al.* [21]. The bound states of the weakly bound OH-He complex were spectroscopically investigated by Han and Heaven [22]. The depolarization of rotationally excited OH radicals with He under thermal conditions has been studied using two-color laser spectroscopy by Paterson *et al.* [23].
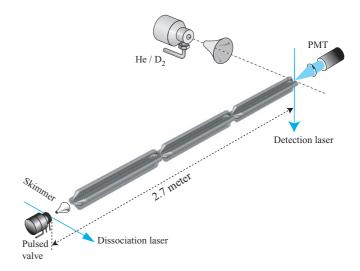

FIG. 1. (Color online) Scheme of the experimental setup. A pulsed beam of OH radicals is produced via photodissociation of HNO$_3$ seeded in an inert carrier gas. The OH radicals pass through a 2.6-m-long Stark decelerator, and are scattered with a pulsed beam of He atoms or D$_2$ molecules. The OH radicals are state-selectively detected via laser-induced fluorescence, that is recorded with a photomultiplier tube (PMT).

All these experiments have been in good agreement with theoretical calculations based on accurate *ab initio* potential energy surfaces [24–26]. The interaction between OH radicals and D$_2$ molecules has been studied less extensively. In crossed beam experiments, inelastic as well as reactive scattering processes have been studied at high collision energies [27–29]. The system has recently been treated theoretically using the quasiclassical trajectory method [30]. Rotational inelastic cross sections for the related OH-H$_2$ system have been calculated by Van Dishoeck and co-workers [31].

II. EXPERIMENT

The experiments are performed in a crossed molecular beam machine that is schematically shown in Fig. 1. This machine has been used recently to study the rotational energy transfer in collisions between state-selected OH ($X\,^2\Pi_{3/2}, J = 3/2, f$) radicals and Ar atoms as a function of the collision energy [16]. A detailed description of the production, Stark deceleration and detection of the OH radicals, as well as of the procedure that is followed to tune the collision energy is given in Ref. [16]; we here limit ourselves to a brief summary.

A pulsed supersonic beam of OH radicals in the $X\,^2\Pi_{3/2}, J = 3/2$ state is produced by photolysis of nitric acid seeded in an inert carrier gas. The OH radicals that reside in the upper Λ-doublet component of f parity are decelerated, guided, or accelerated with the use of a 2.6-m-long Stark decelerator that is used in the so-called $s = 3$ operation mode [15,32]. The OH radicals are scattered with a neat beam of He atoms or D$_2$ molecules at a distance of 16.5 mm from the exit of the decelerator. The beams scatter under 90° angle of incidence and collisions take place in a field free region. The density of the He and D$_2$ molecular beams are kept sufficiently low to ensure single collision conditions.

The beam of D$_2$ molecules is produced using a gas of normal D$_2$, and both ortho-D$_2$ and para-D$_2$ molecules contribute
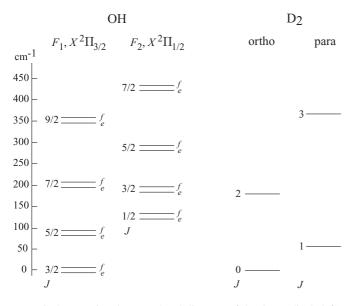
FIG. 2. Rotational energy level diagram of the OH radical (left) and the D_2 molecule (right). The rotational states are labeled with the rotational quantum number J. The spectroscopic symmetry labels e and f are used to denote the two Λ-doublet components that exist for every rotational state of OH. The splitting between both components is largely exaggerated for reasons of clarity.

therefore to the measured state-to-state inelastic cross sections. According to the statistical weights, 67% and 33% of the D_2 molecules are expected to reside in a rotational state belonging to ortho and para-D_2, respectively. The rotational energy level diagram of D_2 is schematically shown in Fig. 2. The energy level spacing between the lowest rotational states is large, and the D_2 molecules are expected to predominantly reside in the $J = 0$ and the $J = 1$ levels under our experimental conditions.

The collision energy is varied by tuning the velocity of the OH radicals, and by choosing different temperatures for the solenoid valve used to produce the He and D_2 beams. The mean forward velocity of the He and D_2 beam is measured by two microphone based beam detectors placed 300 mm apart. For a given temperature of the valve, similar beam speeds are measured for He and D_2 as is to be expected for beam particles of identical mass. The lowest collision energies are obtained when the solenoid valve is cooled to near liquid nitrogen temperatures, resulting in a minimum mean beam velocity of 996 m/s for He and 1042 m/s for D_2. These velocities are expected for particles with a mass of 4 atomic units and near liquid nitrogen nozzle temperatures. The slightly higher speeds that are measured for D_2 beams are attributed to the extra degrees of freedom of the D_2 rotor compared to He.

The lowest collision energy amounts to 120 cm^{-1} and 150 cm^{-1} for OH-He and OH-D_2, respectively. In the experiment by Sawyer *et al.*, a minimum collision energy of ~60 cm^{-1} for OH-He and ~145 cm^{-1} for OH-D_2 was obtained [17]. It is noted that the significantly lower collision energy for OH-He that was reached in that experiment is not due to the use of trapped OH radicals. A center of mass collision energy of ~60 cm^{-1} for collisions between stationary OH radicals and helium atoms requires a He atom velocity of

~670 m/s. This is much lower than the expected velocity for a supersonic beam of helium atoms at the temperature used, and the atomic beam that was employed by Sawyer *et al.* is believed to have been effusivelike [33].

Collision energies up to 400 cm^{-1} for OH-He and 500 cm^{-1} for OH-D_2 are reached by tuning the velocity of the OH radicals between 168 and 741 m/s, and by using temperatures of 293 K, 253 K, 213 K, 173 K, 133 K, and 93 K for the valve producing the He or D_2 beam. The width (full width at half maximum) of the collision energy distribution depends on the velocity distribution and angular spreads of both beams. These are accurately known for the OH radicals from simulations of the deceleration process; for the He and D_2 beams these are estimated from the microphone measurements. The collision energy distribution ranges from ~20 cm^{-1} at the lowest collision energies to ~60 cm^{-1} at the highest collision energies.

Collisional excitation of the OH radicals up to the $X\,^2\Pi_{3/2}, J = 9/2$ and the $X\,^2\Pi_{1/2}, J = 7/2$ state is measured. These rotational states are schematically shown in the rotational energy level diagram in Fig. 2, and are referred to hereafter as $F_i(Je\text{-}f)$, where $i = 1$ and $i = 2$ are used to indicate the $X\,^2\Pi_{3/2}$ and the $X\,^2\Pi_{1/2}$ spin-orbit manifolds, respectively. The inelastically scattered OH radicals are state-selectively detected via saturated laser induced fluorescence using different rotational transitions of the $A\,^2\Sigma^+, v = 1 \leftarrow X\,^2\Pi, v = 0$ band. The off-resonant fluorescence is collected at right angles and imaged into a photomultiplier tube (PMT). The diameter of the laser beam is approximately 8 mm, providing a detection volume that is larger than the intersection volume of both beams.

The experiment runs at a repetition rate of 10 Hz. The beam that provides the collision partner is operated every second shot of the experiment, and the collision signal results as the signal intensity difference of alternating shots of the experiment. The collision energy is varied in a quasicontinuous cycle, as has been described in detail in Ref. [16]. For the strongest scattering channels, the fluorescence signals are recorded using an analog mode of detection; the weak signals are analyzed using photon counting. Both modes of signal acquisition are calibrated with respect to each other.

To relate the measured signal intensities to collision induced populations, the different excitation rates for the different branches of the optical transitions used to probe the different rotational levels are taken into account in the data analysis [16]. The measured relative populations in the various rotational states directly reflect inelastic cross sections. No density-to-flux transformation is required for crossed beam scattering experiments using a light particle as collision partner [34]. The validity of this assumption is verified by a measurement of the variation of the relative collision signals as a function of time in the overlapping beams. No variation was recorded in the experiment, in agreement with model calculations of the detection probabilities of the scattered molecules.

We now describe the theoretical methods used to calculate the cross sections for the inelastic scattering between OH radicals and He atoms; a discussion of the experimental relative cross sections is given in Sec. IV.

III. THEORY

Fully quantum, close-coupling scattering calculations of inelastic collisions of OH radicals with He atoms have been performed recently by Kłos *et al.* in Ref. [35] based on the RCCSD(T) potential energy surfaces of Lee *et al.* [25]. Kłos *et al.* in Ref. [35] present cross sections for rotational transitions out of the $F_1(3/2e)$ state; for the present experiment transitions out of the $F_1(3/2f)$ states are of relevance. Below we briefly describe the scattering methodology relevant for the OH-He system and some of the details of the calculations presented in Ref. [35].

The interaction between the open shell OH($X\,^2\Pi$) radical and a spherical He atom is described by two PES's $V_{A'}$ and $V_{A''}$, having A' and A'' reflection symmetry in the plane containing the OH radical and the He atom [36]. The PES of A' and A'' symmetry describes the OH-He interaction where the OH radical has its singly occupied π orbital in and perpendicular to the triatomic plane, respectively. In scattering calculations it is more convenient to construct the average potential $V_{\rm sum} = 1/2(V_{A''} + V_{A'})$ and the half-difference potential $V_{\rm dif} = 1/2(V_{A''} - V_{A'})$ of these PES's [36,37]. The HIBRIDON program suite was used to carry out fully-quantum, close-coupling calculations of integral state-to-state scattering cross sections [38]. The channel basis was chosen to ensure convergence of the integral cross sections for all $J, F_i \rightarrow J', F_i'$ transitions with $J, J' \leqslant 11.5$. The calculated inelastic cross sections were converged to within 0.01 Å^2.

IV. RESULTS AND DISCUSSION

In Figs. 3 and 4, the measured relative state-to-state inelastic scattering cross sections to levels in the F_1 manifold (spin-orbit conserving collisions) and the F_2 manifold (spin-orbit changing collisions), respectively, are shown. The cross sections that are obtained for the collision partners He and D$_2$ are displayed in the left and right hand side of these figures respectively. The scattering channels that correspond to excitation of the OH radicals to the two different Λ-doublet components of a given rotational state are grouped together. In the upper panels, the scattering channel that populates the $F_1(3/2e)$ state is shown together with the channels that populate both Λ-doublet components of the $F_1(5/2)$ rotational state. To facilitate a direct comparison between the scattering cross sections for OH-He and OH-D$_2$, identical axes are used in the panels that correspond to the same scattering channels. The theoretically calculated cross sections for the scattering of OH with He, convoluted with the experimental energy resolution, are included as solid curves in the left panels.

A. OH-He

In the collision energy range that is probed, the rotational inelastic scattering of OH **($F_1(3/2f)$)** radicals with He atoms is dominated by excitation to the $F_1(5/2e)$ state. The $F_1(3/2e)$ channel, corresponding to collisions that induce the $J = 3/2, f \rightarrow J = 3/2, e$ Λ-doublet transition in the OH radical, appears rather weak. This is in contrast with the scattering of OH radicals with Ar and Xe atoms for which the $F_1(3/2e)$ channel is the dominant inelastic scattering channel [10,16]. The scattering channel populating the $F_2(1/2e)$ state appears
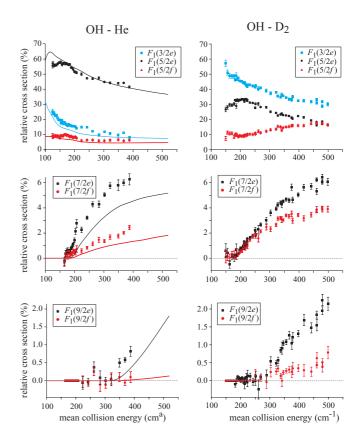

FIG. 3. (Color) Relative state-to-state inelastic scattering cross sections for spin-orbit conserving ($F_1 \rightarrow F_1$) collisions of OH ($X\,^2\Pi_{3/2}, J = 3/2, f$) radicals with helium atoms (left) and D$_2$ molecules (right). The theoretically calculated cross sections for the scattering of OH with He from Ref. [35] are included as solid curves in the left panels.

exceptionally large, also at variance with the corresponding cross sections for the collision partners Ar and Xe.

For spin-orbit manifold conserving collisions, there is a strong propensity for final states of e parity. For spin-orbit manifold changing collisions populating the $J = 1/2$ and $J = 3/2$ states, very strong propensities are observed, showing a near symmetry selection rule. Collisions that populate the $F_2(1/2e)$ and $F_2(3/2f)$ states are approximately two orders of magnitude more effective than collisions populating the $F_2(1/2f)$ and $F_2(3/2e)$ states, respectively.

At high collision energies, the relative state-to-state cross sections and the propensities are consistent with the observations by Schreel *et al.* [20]. In that experiment, however, the strong propensities were partially concealed due to a sizable initial population in the $F_1(5/2f)$ state [20]. The almost perfect quantum state purity of the packets of OH radicals that are used in the present experiment enables to unambiguously measure the cross sections of transitions to final states that are only weakly coupled to the $F_1(3/2f)$ initial state.

The energy range that is probed encompasses the energetic thresholds for scattering into all rotationally excited states, except for the scattering into the $F_1(5/2e)$ and $F_1(5/2f)$ states which open at a collision energy of 84 cm^{-1}. Throughout the range of collision energies, a good agreement is found with the computed cross sections. The relative scattering
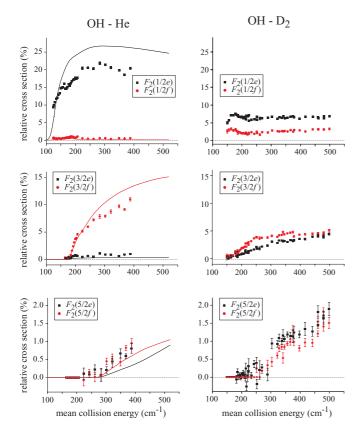
FIG. 4. (Color) Relative state-to-state inelastic scattering cross sections for spin-orbit changing ($F_1 \rightarrow F_2$) collisions of OH ($X\,^2\Pi_{3/2}, J = 3/2, f$) radicals with helium atoms (left) and D_2 molecules (right). The theoretically calculated cross sections for the scattering of OH with He from Ref. [35] are included as solid curves in the left panels.

TABLE I. Values of the coefficients A^l and B^l for excitation of OH ($X\,^2\Pi_{3/2}, J = 3/2, f$) radicals into the lowest lying rotational states (values reproduced from Ref. [39]).

Final state			Λ-doublet transition			
			$f \rightarrow f$		$f \rightarrow e$	
	J	l	A^l	B^l	A^l	B^l
F_1	$\frac{3}{2}$	0	-0.50	0	0	0
		1	0	0	-0.38	0
		2	-0.21	0.11	0	0
		3	0	0	-0.07	0
F_1	$\frac{5}{2}$	1	0.26	0	0	0
		2	0	0	0.28	0.09
		3	0.19	-0.09	0	0
		4	0	0	0.07	0.01
F_2	$\frac{1}{2}$	1	-0.07	0	0	0
		2	0	0	-0.06	0.44
F_2	$\frac{3}{2}$	1	0	0	0.05	0
		2	0.08	0.30	0	0
		3	0	0	0.06	-0.27

cross sections, the propensities for transitions to one of the Λ-doublet components of the final rotational state, as well as the threshold behavior of the various channels are reproduced well. The largest difference between theory and experiment is found for the $F_2(1/2e)$ channel.

The scattering calculations provide quantitatively the state-to-state scattering cross sections, but do not reveal the physical origin of the general behavior of the scattering cross sections and in particular the Λ-doublet propensities. A general analysis of the scattering of $^2\Pi$ molecules with spherical objects has been developed by Dagdigian *et al.* [39], and can be used to qualitatively understand the inelastic scattering of OH radicals with atomic collision partners [24,40]. From the formal quantum analysis of the scattering, it follows that the coupling between rotational states can be evaluated from

$$\sum_l K^l \left[A^l_{\Omega'J'\epsilon',\Omega J\epsilon} V_{l0} + B^l_{\Omega'J'\epsilon',\Omega J\epsilon} V_{l2} \right], \quad (1)$$

where J is the rotational quantum number of the OH radical, ϵ is the symmetry index of the rotational state, and Ω is the projection of J onto the internuclear axis. Primed quantum numbers indicate the postcollision conditions. The terms V_{l0} and V_{l2} are the expansion coefficients of the average and difference potentials in terms of regular and associated Legendre polynomials, respectively. The sum in Eq. (1) is performed over the expansion index l.

The factor K^l is only nonzero for states that are coupled by the interaction potential, and needs for our analysis no further discussion. Essential in the understanding of the inelastic cross sections are the values for the V_{l0} and the V_{l2} coefficients, and the role of the A^l and B^l factors. Both A^l and B^l are independent of the interaction potential, and are determined exclusively by the rotational energy level structure of the molecule. The values of A^l and B^l for OH radicals in the $X\,^2\Pi_{3/2}, J = 3/2, f$ level are tabulated in Ref. [39], and are reproduced in Table I for excitation into the four lowest lying rotational states.

For a pure Hund's case (a) molecule, the values for B^l are zero for spin-orbit manifold conserving collisions, whereas the factors A^l are zero for spin-orbit manifold changing collisions. Consequently, spin-orbit conserving and spin-orbit changing transitions are induced exclusively by V_{sum} and V_{dif}, respectively. Within each manifold, e-f parity changing collisions are governed by the terms for which $\Delta J + l =$ odd, while e-f parity conserving collisions are described by the $\Delta J + l =$ even terms. The propensities for preferred excitation to the e or f component of a final rotational state originate from the different values for the relevant products $A^l V_{l0}$ or $B^l V_{l2}$ that govern these transitions.

For molecules like OH that cannot be described by a pure Hund's case (a) coupling scheme, both the factors A^l and B^l are nonzero, and interference between the average and difference potentials occurs. The $X\,^2\Pi$ electronic ground state of the OH radical originates from a π^3 electron occupancy, leading to predominantly positive values for V_{sum} and V_{dif} [24,39]. As a result, final states for which the dominant A^l and B^l factors have equal signs are coupled more strongly to the $F_1(3/2f)$ initial state than final states for which A^l and B^l have opposite signs. The former is the case for the final states of e parity in the F_1 spin-orbit manifold, and for final states of f parity

in the F_2 manifold, contributing to the observed propensities. The anomalous propensity that is observed for the $F_2(1/2e)$ state can be understood from Eq. (1). Excitation into the $F_2(1/2f)$ state is governed exclusively by V_{10} in combination with a small value for A ($A = -0.07$), while the V_{22} term in combination with a large value for B ($B = 0.44$) dominates the excitation into the $F_2(1/2e)$ state [24,39]. As pointed out by Esposti *et al.* the qualitative analysis given above works well for excitation into rotational states with low J only; for excitation to higher J a qualitative analysis based exclusively on the A^l and B^l coefficients is not straightforward [24].

The measured relative state-to-state cross sections directly yield qualitative information on the expansion coefficients of the potential energy surfaces that govern the scattering between OH and He. Collisions that populate the $F_1(3/2e)$ and $F_1(5/2f)$ states are governed by the coefficients for which $l =$ odd, while the cross sections for excitation to the $F_1(5/2e)$ state is governed by the $l =$ even coefficients. The observed ratio of the state-to-state cross sections indicates that the leading $l =$ even terms V_{20}, V_{40}, and V_{22} contribute significantly to the interaction potential. The relatively large cross section for spin-orbit changing collisions populating the $F_2(1/2e)$ state, as well as the strong propensities that are generally observed, suggests that the V_{22} coefficient of the difference potential plays a significant role in the scattering between OH radicals and He atoms. These effects can be rationalized by the nature of the OH-He interaction potential. The interaction between OH and He is rather weak and the anisotropy of the potential energy surface is small. The $V_{A''}$ PES has two shallow and almost equally deep potential wells for the collinear OH-He and the HO-He geometry, with well depths of 27 cm^{-1} and 22 cm^{-1}, respectively [25]. Consequently, the $l =$ even coefficients that describe the head-tail symmetric parts of the potential energy surfaces contribute significantly to the scattering.

B. OH-D$_2$

The inelastic scattering of OH radicals with D$_2$ molecules shows interesting differences compared to OH-He. The largest cross section is observed for collisions that populate the $F_1(3/2e)$ state. For the channels that populate the $F_1(5/2)$ states, a propensity for the Λ-doublet component of e symmetry is observed for low collision energies, that vanishes for collision energies of about 500 cm^{-1}. The other scattering channels show only modest propensities. The spin-orbit changing collisions appear rather weak.

Although the formalism that was applied above to the scattering of OH with He does not strictly apply to non-spherical collision partners, we can use the formalism to obtain a physical interpretation of the differences between the scattering of OH with He and D$_2$. This comparison is particularly interesting, as both collision partners have equal mass, and mass effects in the dynamics cancel. The interaction of D$_2$ molecules with OH radicals is stronger and induction forces are more important than for the interaction between OH and He. This suggests that the PES is less head-tail symmetric in comparison to OH-He, and the coefficients of the potential for which $l =$ odd gain importance compared to the $l =$ even coefficients. This results in a larger cross section for Λ-doublet changing collisions populating the $F_1(3/2e)$ state, smaller spin-orbit changing transitions, and

less pronounced propensities for preferred excitation to one of the two components of a Λ doublet. Similar effects have been observed in state-to-state inelastic scattering experiments of OH radicals with polar collision partners such as HCl [41], HBr [42] and HI [43], and also CO$_2$ [44].

In the relative inelastic scattering cross sections, no effect is seen from the internal rotational degrees of freedom of the D$_2$ molecule. In particular, no strong variation of the cross sections at collision energies around 300 cm^{-1} is observed, that could be indicative of resonant energy transfer between the OH and the D$_2$ rotors [17].

V. CONCLUSIONS

We have presented measurements of the state-to-state rotational inelastic scattering of Stark-decelerated OH ($X\,^2\Pi_{3/2}, J = 3/2, f$) radicals with He atoms and D$_2$ molecules in the 100–500 cm^{-1} collision energy range. The collision energy dependence of the relative inelastic scattering cross sections, the threshold behavior of inelastic channels, and the energy dependence of the state-resolved propensities are accurately determined. For the scattering of OH with He, good agreement is found with the inelastic scattering cross sections determined from quantum close-coupled scattering calculations based on high-quality *ab initio* OH-He PES's.

The almost perfect quantum state purity of the Stark-decelerated packets of OH radicals eliminates the contamination of the scattering signals by initial populations in excited rotational states. This facilitates a quantitative study of collision induced transitions to states that are only weakly coupled to the initial state, and enables the observation of the exceptionally strong propensities for the inelastic scattering between OH radicals and He atoms. The genuine relative state-to-state inelastic scattering cross sections that are measured allow for an accurate comparison with computed cross sections.

Significant differences are found between the inelastic scattering of OH-He and OH-D$_2$. Although no rigorous quantum calculations have been performed for OH-D$_2$, these differences can be understood from the different nature of the OH-D$_2$ interaction potential. No effect of the rotational degrees of freedom of the D$_2$ molecule has been observed in the relative inelastic scattering cross sections.

Our measurements on the low-energy scattering between OH radicals and He or D$_2$ complement recent scattering experiments in which pulsed beams of He or D$_2$ are directed through a sample of magnetically trapped OH radicals. In that experiment, inelastic collisions, as well as elastic collisions that impart a sufficient amount of kinetic energy to the OH radicals, lead to a reduced number of OH radicals in the trap. Recent quantum scattering calculations, based on the same PES's as used in the present work, have not been able to reproduce the trap loss observations for OH-He, however. The state-to-state experiments reported in the present article are not sensitive to elastic scattering, but validate the field-free inelastic scattering cross sections for OH-He determined from quantum scattering calculations. The theoretical description of low-energy inelastic collisions of these elementary systems is thus adequate; more experimental and theoretical work is needed to find the source of the discrepancy between theory

and beam-trap experiments. For the accurate interpretation of collision experiments using trapped molecules, it is essential to establish the role of elastic scattering and the influence of the trapping potential on the measured trap loss.

Note added in proof. Recent calculations by Tscherbul *et al.* [45] suggest that trapping fields can have a large effect on the measured trap loss in beam-trap experiments, and that the trap loss that was observed by Sawyer *et al.* [17] for the scattering of OH radicals with He atoms is dominated by elastic scattering.

[1] M. T. Bell and T. P. Softley, Mol. Phys. **107**, 99 (2009).

[2] I. W. M. Smith, Angew. Chem. Int. Ed. **45**, 2842 (2006).

[3] *Focus on Cold and Ultracold Molecules*, edited by L. Carr and J. Ye (special issue in New Journal of Physics, 2009).

[4] *Low Temperatures and Cold Molecules*, edited by I. W. M. Smith (Imperial College Press, London, 2008).

[5] *Cold Molecules: Theory, Experiment, Applications*, edited by R. V. Krems, W. C. Stwalley, and B. Friedrich (Taylor and Francis, New York, 2009).

[6] D. W. Chandler, J. Chem. Phys. **132**, 110901 (2010).

[7] R. V. Krems, Phys. Chem. Chem. Phys. **10**, 4079 (2008).

[8] K. Maussang, D. Egorov, J. S. Helton, S. V. Nguyen, and J. M. Doyle, Phys. Rev. Lett. **94**, 123002 (2005).

[9] W. C. Campbell, T. V. Tscherbul, Hsin I. Lu, E. Tsikata, R. V. Krems, and J. M. Doyle, Phys. Rev. Lett. **102**, 013003 (2009).

[10] J. J. Gilijamse, S. Hoekstra, S. Y. T. van de Meerakker, G. C. Groenenboom, and G. Meijer, Science **313**, 1617 (2006).

[11] S. Willitsch, M. T. Bell, A. D. Gingell, S. R. Procter, and T. P. Softley, Phys. Rev. Lett. **100**, 043203 (2008).

[12] S. Ospelkaus, K. K. Ni, D. Wang, M. H. G. de Miranda, B. Neyenhuis, G. Quemener, P. S. Julienne, J. L. Bohn, D. S. Jin, and J. Ye, Science **327**, 853 (2010).

[13] K. K. Ni, S. Ospelkaus, D. Wang, G. Quéméner, B. Neyenhuis, M. H. G. de Miranda, J. L. Bohn, J. Ye, and D. S. Jin, Nature (London) **464**, 1324 (2010).

[14] S. Y. T. van de Meerakker, H. L. Bethlem, and G. Meijer, Nature Physics **4**, 595 (2008).

[15] L. Scharfenberg, H. Haak, G. Meijer, and S. Y. T. van de Meerakker, Phys. Rev. A **79**, 023410 (2009).

[16] L. Scharfenberg, J. Kłos, P. J. Dagdigian, M. H. Alexander, G. Meijer, and S. Y. T. van de Meerakker, Phys. Chem. Chem. Phys. **12**, 10660 (2010).

[17] B. C. Sawyer, B. K. Stuhl, D. Wang, M. Yeo, and J. Ye, Phys. Rev. Lett. **101**, 203203 (2008).

[18] Z. Pavlovic, T. V. Tscherbul, H. R. Sadeghpour, G. C. Groenenboom, and A. Dalgarno, J. Phys. Chem. A **113**, 14670 (2009).

[19] M. Elitzur, Rev. Mod. Phys. **54**, 1225 (1982).

[20] K. Schreel, J. Schleipen, A. Eppink, and J. J. ter Meulen, J. Chem. Phys. **99**, 8713 (1993).

[21] I. J. Wysong, J. B. Jeffries, and D. R. Crosley, J. Chem. Phys. **94**, 7547 (1991).

[22] J. Han and M. C. Heaven, J. Chem. Phys. **123**, 064307 (2005).

[23] G. Paterson, S. Marinakis, M. L. Costen, K. G. McKendrick, J. Kłos, and R. Toboła, J. Chem. Phys. **129**, 074304 (2008); **131**, 159901(E) (2009).

[24] A. Degli Esposti, A. Berning, and H.-J. Werner, J. Chem. Phys. **103**, 2067 (1995).

[25] H.-S. Lee, A. B. McCoy, R. R. Toczyłowski, and S. M. Cybulski, J. Chem. Phys. **113**, 5736 (2000).

[26] P. J. Dagdigian and M. H. Alexander, J. Chem. Phys. **130**, 164315 (2009).

[27] P. Andresen, N. Aristov, V. Beushausen, and H. W. Lülf, J. Chem. Phys. **95**, 5763 (1991).

[28] M. Alagia, N. Balucani, P. Casavecchia, D. Stranges, G. G. Volpi, D. C. Clary, A. Kliesch, and H.-J. Werner, Chem. Phys. **207**, 389 (1996).

[29] B. R. Strazisar, C. Lin, and H. F. Davis, Science **290**, 958 (2000).

[30] J. D. Sierra, R. Martinez, J. Hernando, and M. González, Phys. Chem. Chem. Phys. **11**, 11520 (2009).

[31] A. R. Offer, M. C. van Hemert, and E. F. van Dishoeck, J. Chem. Phys. **100**, 362 (1994).

[32] S. Y. T. van de Meerakker, N. Vanhaecke, H. L. Bethlem, and G. Meijer, Phys. Rev. A **71**, 053409 (2005).

[33] B. C. Sawyer (private communication).

[34] D. M. Sonnenfroh and K. Liu, Chem. Phys. Lett. **176**, 183 (1991).

[35] J. Kłos, F. Lique, and M. H. Alexander, Chem. Phys. Lett. **445**, 12 (2007).

[36] M. H. Alexander, Chem. Phys. **92**, 337 (1985).

[37] M. H. Alexander, J. Chem. Phys. **76**, 5974 (1982).

[38] HIBRIDON is a package of programs for the time-independent quantum treatment of inelastic collisions and photodissociation written by M. H. Alexander, D. E. Manolopoulos, H.-J. Werner, B. Follmeg, and others. More information and/or a copy of the code can be obtained from the website [http://www2.chem.umd.edu/groups/alexander/hibridon/hib43].

[39] P. J. Dagdigian, M. H. Alexander, and K. Liu, J. Chem. Phys. **91**, 839 (1989).

[40] M. C. van Beek, J. J. ter Meulen, and M. H. Alexander, J. Chem. Phys. **113**, 628 (2000).

[41] R. Cireasa, M. C. van Beek, A. Moise, and J. J. ter Meulen, J. Chem. Phys. **122**, 074319 (2005).

[42] A. Moise, R. Cireasa, D. H. Parker, and J. J. ter Meulen, J. Chem. Phys. **125**, 204315 (2006).

[43] A. Moise, D. H. Parker, and J. J. ter Meulen, J. Chem. Phys. **126**, 124302 (2007).

[44] M. C. van Beek, K. Schreel, and J. J. ter Meulen, J. Chem. Phys. **109**, 1302 (1998).

[45] T. V. Tscherbul, Z. Pavlovic, H. R. Sadeghpour, R. Côté, and A. Dalgarno, Phys. Rev. A **82**, 022704 (2010).